Hybodontiform sharks from Middle Triassic Chang 7 Member of the Ordos Basin, Shaanxi, North China: palaeobiological and palaeoecological significances

Jia-Chun Li, Zuo-Yu Sun, Gilles Cuny, Qing-Qiang Meng, Da-Yong Jiang

Hybodontiform sharks from Middle Triassic Chang 7 Member of the Ordos Basin, Shaanxi, North China：palaeobiological and palaeoecological significances

Li Jiachun[a, b], Sun Zuoyu[b, *], Gilles Cuny[c], Meng Qingqiang[d, *] and Jiang Dayong[b]

[a]State Key Laboratory of Shale Oil and Gas Enrichment Mechanisms and Effective Development, Beijing 102206, China

[b]Laboratory of Orogenic Belt and Crustal Evolution, Ministry of Education, Department of Geology and Geological Museum, Peking University, Yiheyuan Street 5, Beijing100871, China <lijiachun@pku.edu.cn; sunzuoyu@pku.edu.cn; djiang@pku.edu.cn>

[c]Univ Lyon, Université Claude Bernard Lyon 1, CNRS, ENTPE, UMR 5023 LEHNA, F-69622, Villeurbanne, France <gilles.cuny@univ-lyon1.fr>

[d]Petroleum Exploration and Production Research Institute, China Petroleum and Chemical Corporation, Beijing 100088, China <mengqq.syky@sinopec.com>

*Corresponding authors.

Abstract.—The lacustrine ecosystem of the early Ladinian of Chang 7 Member of Yanchang Formation in the Ordos Basin (Shaanxi, North China) was proposed as the earliest known Mesozoic-type, trophically multileveled lacustrine ecosystem after the end-Permian mass extinction (EPME). However, the sharks being top predators was a mere conjecture from coiled coprolites. Herein, thirty-one shark teeth from the organic-rich mudstones of the Chang 7 Member at the Bawangzhuang section, Tongchuan City, Shaanxi Province, North China are described in details. Two taxa of hybodontiformes, *Hybodus? youngi* and *Hybodus*

sp., are identified. Based on new material and a reexamination of original material, the previously described *Hybodus? youngi* is substantially revised by adding several newly recognized anatomical features that include flared lateral cusplets, orthodont crown with a pulp cavity surrounded by numerous dentine tubules and a monognathic heterodonty. The results indicate that at least two different hybodont sharks, associated with *Saurichthys* of ca. 1 m in total length, occupied the higher trophic levels of the Chang 7 Member's lacustrine ecosystem. The re-establishment of large predator niches encompassing diverse large predators with multiple dietary habits further supports a full recovery of the lacustrine ecosystem structure 10 Myr after the EPME.

Keywords: Hybodontiform; lacustrine ecosystem; Middle Triassic; Chang 7 Member; North China.

1. Introduction

The Ordos Basin, the largest intracontinental sedimentary basin in China (Du et al., 2019), has a huge petroliferous resource potential that would cover about one third of China's total oil and gas production (Yang et al., 2013). In particular, lacustrine organic-rich shales and mudstones of the Middle Triassic Chang 7 Member of the Yanchang Formation (Deng et al., 2018; Zhao et al., 2020) are the dominant high-quality hydrocarbon source rocks among Mesozoic oil pools of the Ordos Basin (Qiu et al., 2015). Accordingly, Chang 7 Member has attracted increasing attention from the scientific community, and thus its sedimentology, petrology, organic geochemistry and palaeontology have been extensively studied (Liu et al., 2021 and reference therein). Fossils of micro/macroalgae, notostracans, ostracods, plants,

bony fishes, sharks and fish coprolites were recorded in different locations of Chang 7 (Liu, 1962; Jin, 2006; Yang et al., 2013, 2016). Recently, the Chang 7 Member's lacustrine ecosystem was reconstructed based on its fossil records from four sections (i.e., Bawangzhuang, Mazhuang, Yishicun and Qishuihe), Tongchuan City, Shaanxi Province, North China (Zhao et al., 2020). Therein, a Mesozoic-type, trophically multileveled lacustrine ecosystem was proposed as the earliest known complex lacustrine ecosystem following the end-Permian mass extinction (Zhao et al., 2020). However, their key evidence to demonstrate the existence of complex food webs (i.e. 'sharks being top predators') was indirectly inferred from coiled coprolites, which could leave their conclusion open to question as sharks are not the only predator to produce coiled coprolites (Laojumpon et al., 2012).

Here, shark teeth were collected from the organic-rich mudstones of Chang 7 at the Bawangzhuang section, Tongchuan City, Shaanxi Province, North China. Outside Bawangzhuang section, sharks of the Chang 7 were insufficiently known apart from three isolated shark teeth from Ansai, Shaanxi Province (Liu, 1962) that were identified as *Hybodus youngi*. Thus, the aim of the present paper is 1) to describe the new shark teeth, 2) to substantially revise the previously incompletely described *Hybodus youngi* on the basis of new material and a reexamination of original material, and 3) to assess the palaeobiological and palaeoecological significances of the Chang 7 sharks for the reconstruction of the early Ladinian lacustrine ecosystem of the Ordos Basin.

2. Geological setting

The Bawangzhuang section (35°14′2.83″ N, 109°02′28.86″ E) is situated on the southern margin of the Ordos Basin, approximately 5 km to Jinsuoguan Town, Tongchuan City, Shaanxi Province, North China (Fig. 1A, B). The Ordos Basin is a non-marine basin that was deposited on the Palaeozoic North China Craton. The Triassic of the Ordos Basin is characterized by, in ascending order, the Early Triassic and early Middle Triassic mostly fluvial deposits of the Liujiagou Formation, Heshanggou Formation and Ermaying Formation, and the late Middle Triassic and Late Triassic mostly lacustrine successions of the Tongchuan Formation and Yanchang Formation (IGCAGS, 1980). The last two formations (approximately equal to the Yanchang Group or Formation cited by Yang et al., 2000; Li et al., 2016; Deng et al., 2018) represent the main oil-bearing series and are further subdivided into 10 oil reservoir units, named Chang 10 to Chang 1 members from bottom to top (Qiu et al., 2010; Deng et al., 2018). The Chang 7 Member comprises organic-rich shales and mudstones with a total thickness of 100-120 m (Qiu et al., 2015; Deng et al., 2018). The Bawangzhuang section displays the lower part of the Chang 7 Member, with a continuous succession of thick-bedded siltstones, organic-rich shales with abundant tuffs and a carbonate concretion layer, and mudstones (Fig. 1C). The shark teeth described herein, associated with abundant, diverse fish coprolites and bony fish fossils, were collected from the mudstones that lies ca. 10 m above the basal thick-bedded siltstones (Figs. 1C, D). U-Pb isotopic data from the underlying tuff sample indicates an age of 240.3 Ma, within the Ladinian in the late Middle Triassic (Zhao et al., 2020).

3. Materials and methods

The material investigated in this work consists of thirty-one isolated shark teeth. They were collected when we split a huge bulk (ca. 800 kg) of mudstones into thin layers and then carefully observed every bedding surface using magnifying glasses during field works in November 2020 and April 2021. Accordingly, most of them were represented by part and counterpart, respectively. In the laboratory, all samples were prepared using air scribes under binocular microscopes, with the exception of some teeth that were seriously weathered. Pictures of the fossils were taken using a system including a stereo microscope (i.e., Nikon SMZ 25 equipped with a CFI60-2 objective lens for industrial microscopes) and digital camera, and then edited with the software Adobe Photoshop CC 2018. Two teeth were used for histological studies without prior acid-etching using a FEI QUANTA-650FEG SEM with an acceleration voltage of 13 kV. They were washed with a KQ-50TDE ultrasonic cleaner for 15 minutes and then coated with a 20 nm thick chromium layer. The above-mentioned analyses were conducted at the Laboratory of Orogenic Belt and Crustal Evolution, Peking University, China. The systematic framework and terminology used for the description of teeth follow Cappetta (2012). The histological terminology follows Jambura et al., (2020).

Repositories and institutional abbreviations.—The specimens studied here are stored in the collections of GMPKU (Geological Museum of Peking University, Beijing, China). The original material of *Hybodus antingensis* Liu, 1962, *Hybodus huangnidanensis* Wang, 1977 and *Hybodus youngi* Liu, 1962 from the IVPP (Institute of Vertebrate Paleontology and Paleoanthropology, Chinese Academy of Sciences) collection were re-examined for comparisons.

4. Systematic palaeontology

(by JC Li and G Cuny)

Class Chondrichthyes Huxley, 1880

Subclass Elasmobranchii Bonaparte, 1838

Cohort Euselachii Hay, 1902

Order Hybodontiformes Patterson, 1966

Family Hybodontidae Owen, 1846

Genus *Hybodus* Agassiz, 1837

Type species.—*Hybodus reticulatus* Agassiz, 1837, by original designation, from the Lower Jurassic, Lyme Regis, England.

Hybodus? youngi Liu, 1962

Figures 2, 3A-I

1962 *Hybodus youngi* Liu, p. 150-156, pl. 1, fig. 2-3.

Type specimens.—Holotype, IVPP V 1042. 1: a tooth from Chang 7 Member, Yanchang Formation (Middle Triassic) of Zhangjiatan, Yanchang County, Yan'an City, Shaanxi Province, North China. Holotype, IVPP V 1042. 1 (Liu, 1962, pl. 1, fig. 2; Fig. 3G); Paratypes, IVPP V 1042. 2 (Liu, 1962, pl. 1, fig. 3, left; Fig. 3H) and IVPP V 1042. 3 (Liu, 1962, pl. 1, fig. 3, right; Fig. 3I).

Material.—Twenty-nine teeth, i.e. GMPKU-P-3613a/b, GMPKU-P-3615a/b~3619a/b, GMPKU-P-3620~3622, GMPKU-P-3625, GMPKU-P-3627, GMPKU-P-3629, GMPKU-P-3642a/b~3646a, GMPKU-P-3647, GMPKU-P-3648a/b~3649a/b, GMPKU-P-3650~3651, GMPKU-P-3652a/b, GMPKU-P-3654a/b~3656a/b, GMPKU-P-3657, GMPKU-P-3659 and GMPKU-P-3661. Specimens used for imaging: GMPKU-P-3613a, GMPKU-P-3615a, GMPKU-P-3617a, GMPKU-P-3619a, GMPKU-P-3620, GMPKU-P-3625, GMPKU-P-3627, GMPKU-P-3642a, GMPKU-P-3643a, GMPKU-P-3644a, GMPKU-P-3645b, GMPKU-P-3646a, GMPKU-P-3648a, GMPKU-P-3649b, GMPKU-P-3650, GMPKU-P-3651, GMPKU-P-3652a, GMPKU-P-3654b and GMPKU-P-3661.

Emended diagnosis.—Symmetrical or asymmetrical teeth with various number of lateral cusplets. Gradual monognathic heterodonty consisting of teeth with relatively high and upright main cusp anterolaterally and lower and inclined main cusp posterolaterally. The main cusp has a rounded apex and is ornamented by numerous (more than nine) vertical ridges both labially and lingually. Lateral cusplets are triangular in outline and flared basally in labial and lingual views. The root is low and nearly straight. Orthodont teeth with numerous dentine tubules extending to the enameloid/dentine junction and a well-developed pulp cavity that is filled by osteodentine in the lower part.

Differential diagnosis with the type species of Hybodus, H. reticulatus.—Main cusp and cusplets less slender with a blunt apex, no well-developed cutting edges, ornamentation

ridges attaining the apex of cusp and cusplets, up to four lateral cusplets on the mesial side, teeth orthodont.

Description.—The teeth measure 3.2-12.0 mm mesiodistally, 1.8-2.1 mm labiolingually and 1.8-6.6 mm in height. A gradient monognathic heterodonty is recognized: the main cusp is high and upright in anterolateral teeth and rather lower and inclined distally in posterolateral teeth. The crown is symmetrical or asymmetrical, displaying a varying number of lateral cusplets. The main cusp is prominent, flanked by one to three lateral cusplets on the distal side and one to four lateral cusplets on the mesial side. The asymmetrical crowns usually have more lateral cusplets on the mesial side than on the distal one (Fig. 2P, R). The main cusp has a height about twice to three times the height of the first pair of lateral cusplets and about half the mesiodistal length of the tooth. In all teeth, the apex of the main cusp is domed and rounded, whereas the lateral cusplets show a bluntly tipped apex. The lateral cusplets are flared mesiodistally, triangular in shape (Figs. 2F, G, 3G, H). The main cusp is separated from the first pair of lateral cusplets by a U-shaped notch that appears to be usually smoother and more elongated on the distal side than on the mesial side (Fig. 2O, P). In apical view, specimen GMPKU-P-3644 and GMPKU-P-3649 show that the lingual face of the main cusp is almost flat, whereas the labial one is convex (Fig. 2J, K). Well-defined ridges ornament the crown surface and are evenly spaced at the base of the crown. In anterolateral teeth, specimen GMPKU-P-3619a/b and GMPKU-P-3651 show that there are ten to fifteen vertical ridges in the main cusp (Fig. 2C, I): some of them extend apicobasally; some are short and confined within the lower or upper part of the cusp in the labial face. In posterolateral teeth, these

ridges usually converge in the apex (Fig. 2L), however the innermost two may merge into one at the middle part of the cusp (Fig. 2S). Specimen GMPKU-P-3625, GMPKU-P-3627, GMPKU-P-3645 GMPKU-P-3649 and GMPKU-P-3650 display nine to eleven ridges on the main cusp and five to eight ridges on the lateral cusplets on the labial side. Lingually, a similar number and density of ridges are identified from the small protrusion along the lingual edge of the cross section (Fig. 2K). The root is low and nearly straight in most of specimens, however the root of some posterolateral teeth is slightly curved under the main cusp (Figs. 2O, P). The root outline is rarely preserved and observed only in specimen GMPKU-P-3613a/b, where the root is 0.3 mm thick and displays two triangular protrusions in the central part of the crown/root junction (Fig. 2P).

Histology.—The teeth comprise enameloid, dentine and a pulp cavity, which is shown in longitudinal section in most specimens. Each cusp is coated by enameloid (Fig. 3.4, 3.6) that is semi-transparent and 30-100 μm thick. The teeth display a central pulp cavity that is encapsulated by a substantial layer of orthodentine. Such a feature is shown in the cross-section of GMPKU-P-3649b, where the inner layer of dentine around the pulp cavity is penetrated by numerous, minute dentine tubules that appear to be arranged radially (Fig. 3A, B). These dentine tubules originate from the pulp cavity and extend near the enameloid/dentine junction, shown in GMPKU-P-3642a (Fig. 3D). The pulp cavity of the main cusp is well-developed, about 120-370 μm in diameter in the middle part of the main cusp. It reaches more than half the height of the main cusp and its base is partially infilled by the osteodentine of the root (Fig. 3E). All porous structures of the tooth are filled with

197 petroleum asphalt (Appendix 1).

198

199 *Remarks.*—The genus *Hybodus,* at least based on isolated teeth, does not correspond to a
200 biological entity and is probably polyphyletic (Cappetta, 2012). Moreover, whether
201 *Polyacrodus* represents a genus separate from *Hybodus* has been particularly discussed and
202 no consensus has been reached (Rees, 2008; Cappetta, 2012). However, *Polyacrodus* appears
203 to be characterized by orthodont teeth whereas the histology of the teeth of most *Hybodus*
204 species remains largely unknown (Stumpf et al., 2021). The type species, *H. reticulatus,*
205 possess nonetheless pseudoosteodont teeth (Maisey, 1987). This could suggest that the teeth
206 described above are closer to *Polyacrodus* than to *Hybodus,* but it is almost impossible to
207 characterize *Polyacrodus* teeth on external morphological characters (Rees, 1998). It is
208 beyond the scope of this paper to discuss the validity of the genus *Polyacrodus,* but in order
209 to take this situation into account, we assigned the teeth described above as *Hybodus? youngi*
210 to highlight that its generic identification is uncertain (Bengston, 1988).
211 The material is assigned to the species *Hybodus? youngi* Liu, 1962 based on the relatively
212 high crown, robust main cusp, strong vertical ridges and well-separated cusps (Liu, 1962;
213 Xue, 1980; Zhang, 2007). These characteristics are encountered in other Mesozoic hybodont
214 taxa, for example *Hybodus* sp. Kato et al., 1995 , *'Polyacrodus'* sp. Rieppel et al., 1996,
215 *Hybodus reticulatus* Delsate et al., 2002*, Hybodus houtianensis* Lu et al., 2005 and *Hybodus*
216 *plicatilis* Manzanares et al., 2018. However, the flared lateral cusplets of *Hybodus? youngi*
217 make it easily distinguishable from the above-mentioned hybodont taxa. Low lateral cusplets
218 with fairly wide bases are also encountered in teeth of *Crassodus* and *Asteracanthus.*

However, in the former the teeth appears to be more bulbous, with a well-developed longitudinal crest and lateral cusplets less well separated from the main cusp (Maisch et al., 2016) whereas in the latter there are strong labial nodes at the base of the crown (Stumpf et al., 2021). It is worth noting that the attribution of the present specimens to *Hybodus? youngi* mainly relies on morphological comparison of anterolateral teeth with the original material of *Hybodus youngi* (Fig. 3G-I) as the latter does not encompass posterolateral teeth. The posterolateral teeth attributed to *Hybodus? youngi* are quite reminiscent of the posterior teeth of *Hybodus* cf. *keuperianus* as figured by Böttcher (2015). However, they are shorter mesiodistally than the latter. In addition, no anterior teeth of *Hybodus (Polyacrodus) keuperianus,* as described by Winkler (1880) and Dorka (2003), have been recovered in the Chang 7 Member's material. The posterolateral teeth of *Hybodus? youngi* are also reminiscent of *Hybodus antingensis* Liu, 1962 (Fig. 3J) because of the combination of the following characters: strong vertical ridges attaining the apex of cusp and cusplets, a rather low crown, cusps with a broad base and blunt apex, and almost straight crown/root boundary. However, *Hybodus antingensis* is so far restricted to the Middle Jurassic of Ansai County, Yan'an City, Shaanxi Province, North China (Liu, 1962; Xue, 1980; Zhang, 2007) and was proposed as a junior synonym of *Hybodus huangnidanensis* Wang, 1977 (Shang et al., 2008). However, *Hybodus huangnidanensis* presents a low root with a series of round foramina labially (Fig. 3K, L). Such a character is unknown in *Hybodus antingensis* and materials herein described due to the poor preservation of their root in all known specimens. As a result, more complete teeth are necessary to demonstrate this possible synonymy. Anyway, even if these posterolateral teeth from the early Ladinian Chang 7 Member appear to be

morphologically closer to *Hybodus antingensis* than to any other known *Hybodus* species, the large temporal gap between them makes its attribution to the Middle Jurassic *Hybodus antingensis* unlikely.

Liu (1962) pointed out that *Hybodus antingensis* differs from *Hybodus youngi* by having a lower crown, not well-separated cusplets and a main cusp that has sparser vertical ridges reaching its apex. However, such differences might easily be explained by a monognathic heterodonty as seen for example in *Egertonodus basanus* described by Maisey (1983). Herein, two morphological tooth types with high to low and upright to inclined main cusp from the same horizon and locality could therefore represent anterolateral and posterolateral teeth of *Hybodus? youngi,* respectively. Another two teeth, GMPKU-P-3620 and 3642a/b possess one pair of lateral cusplets that are slightly lower than the other anterolateral teeth. They may represent the parasymphysial teeth of *Hybodus? youngi*. In such a way, a gradual monognathic heterodont dentition of *Hybodus? youngi* is tentatively identified based on the present material.

Occurrence.—Early Ladinian (Middle Triassic) of Tongchuan City, and Yanchang County, Yan'an City (Liu, 1962), Shaanxi Province, North China.

Hybodus sp.

Figure 4

Material.—Two specimens, i.e. GMPKU-P-3653a/b and GMPKU-P-3660, all of which were used for imaging.

263

264 *Description:*—Teeth measure 10.2-11.3 mm mesiodistally and 4.7-5.1 mm in height. The
265 asymmetric crown consists of one main cusp flanked by one lateral cusplet on the mesial(?)
266 side and two lateral cusplets on the distal(?) side. The main cusp is robust and upright, at least
267 four times as high as the lateral cusplets. All cusps possess a blunt and domed apex that
268 becomes much rounder on the lateral cusplets. The main cusp and the first pair of lateral
269 cusplets are separated by a smooth and elongated notch. The root is low, with a centrally
270 concave outline below the main cusp. The mesial and distal extremities of the root are
271 rounded.

272

273 *Histology.*—The longitudinal section of a tooth (GMPKU-P-3653a/b) shows numerous
274 vascular canals inside the root, 8-9 μm in diameter and infilled with asphaltene sediments.
275 The internal dentine core does not display a pulp cavity but is secondly infilled by a few
276 vascular canals, which resembles the pseudoosteodont tooth histotype *sensu* Jambura et al.
277 (2020). The outer enameloid layer covers the crown and is well-developed at the apex of the
278 main cusp, reaching about 120 μm in thickness.

279

280 *Remarks.*—The specimens share with abraded teeth attributed to *Planohybodus* sp. by
281 Cupello et al., 2012 an important difference in height between the main cusp and the first pair
282 of lateral cusplets. However, our teeth can be separated from the latter specimens because of
283 their weakly-developed lateral cusplets that almost lacks an apex. Some hybodont sharks
284 have a robust main cusp with rather low or no lateral cusplets, such as *Hybodus rapax,*

285 *Hybodus sasseniensis, Homalodontus aplopagus* and *Meristodonoides montanensis,* but
286 display a heterodont dentition (Case, 1978; Mutter et al., 2007, 2008; Bratvold et al., 2018).
287 Thus, these teeth could represent the anterior ones of *Hybodus? youngi* due to the fact they all
288 possess a similar crown with a robust and upright main cusp. However, it is difficult to make
289 it fit with the heterodonty pattern of *Hybodus? youngi* because of its prominent height
290 difference between the main cusp and the first pair of lateral cusplets and weakly-developed
291 lateral cusplets with nearly no apex. Moreover, they display a different histology. Therefore,
292 they are herein tentatively ascribed to *Hybodus* sp. pending more material for a definite
293 determination.
294
295 *Occurrence*.—Early Ladinian (Middle Triassic), Bawangzhang village, Tongchuan City,
296 Shaanxi Province, North China.
297
298 **5. Discussion**
299 **5.1 Taxonomy**
300 As described above, thirty-one shark teeth from the organic-rich mudstones of the Chang 7
301 Member at the Bawangzhuang section, Tongchuan City, Shaanxi Province, North China were
302 attributed to two taxa of hybodontiformes, i.e. *Hybodus? youngi* and *Hybodus* sp. Of them,
303 *Hybodus? youngi* was previously incompletely described based on three poorly-preserved
304 teeth (Liu, 1962). The diagnosis of *Hybodus? youngi* proposed by Liu (1962) that includes
305 “large teeth, relatively high crown, strong vertical ridges and well-separated lateral cusplets”
306 makes *Hybodus? youngi* poorly diagnostic. Herein, twenty-nine teeth and a reexamination of

the original material of *Hybodus youngi* (Figs. 3.7-3.9) allow us to substantially revise its diagnosis by adding several anatomical features previously unknown. Firstly, one of the most important is the presence of flared lateral cusplets well separated from the main cusp. Outside hybodonts, similar flared lateral cusplets are recorded in the ctenacanth *Dracopristis hoffmanorum* Hodnett et al., 2021. Secondly, the tooth histology of *Hybodus? youngi* shows an orthodont crown with a pulp cavity that is surrounded by numerous dentine tubules. Such a histology appears currently restricted to *Palaeobates* and *Polyacrodus* among Hybodontiformes (Stumpf et al., 2021). Although the tooth histology of many *Hybodus* species is so far unknown, this character could question the attribution of this species to the genus *Hybodus.* A full revision of the latter genus is, however, beyond the scope of the present work. Thirdly, teeth of *Hybodus? youngi* display a crown with high and upright main cusps in anterolateral teeth and with low and inclined ones in posterolateral ones, indicating that *Hybodus? youngi* had a monognathic heterodonty. Therefore, the dentition pattern of *Hybodus? youngi* is herein better understood although some characters of their root still need to be confirmed pending more material.

5.2 Palaeoecology

The lacustrine ecosystem of the early Ladinian Chang 7 Member in the Ordos Basin was deemed to be the earliest complex lacustrine ecosystem after the EPME (Zhao et al., 2020). The trophic pyramid was outlined to include primary producers (various micro- and macroalgae) forming the lowest trophic level, primary consumers (some notostracans, ostracods, and insects that fed on algae) and meso-consumer (some predatory insects such as chaoborid larvae) in the middle part of the food web, and predatory fish lying at higher

329 trophic levels (Zhao et al., 2020). The results of the present work provide direct evidence that
330 hybodont sharks are present in the early Ladinian Chang 7 lacustrine ecosystem and can be
331 proposed as large predators in the upper trophic levels. Whether or not the higher-order
332 trophic structure is rebuilt is key for evaluation of the ecosystem recovery after extinction
333 events (Chen and Benton 2012; Scheyer et al., 2014) because large predators in higher
334 trophic levels are highly susceptible to environmental fluctuations and stress (Casini et al.,
335 2012; Steneck 2012). Hybodontiformes is one of the most successful chondrichthyan lineages
336 ranging from the Late Devonian (ca. 361Ma, Ginter et al., 2002; Hairapetian and Ginter 2009)
337 to the Late Cretaceous (ca. 66 Ma, Kriwet and Benton 2004). After the EPME, a sharp faunal
338 turnover happened within chondrichthyans, with marine Palaeozoic stem chondrichthyans
339 (e.g., cladodontomorphs, petalodontiforms, bransonelliforms, eugeneodontiforms) being
340 replaced by the increasingly dominant hybodontiforms and early radiation of the
341 neoselachians (Guinot et al., 2013; Manzanares et al., 2020). In China, hybodont sharks
342 started to invade continental ecosystem in the Late Permian in North China (Wang et al.,
343 2009). Herein, the existence of hybodont sharks in the early Ladinian lacustrine ecosystem of
344 the Ordos Basin, associated with undescribed *Saurichthys* of ca. 1 m in total length and
345 another two different large-sized actinopterygians of ca. 30 cm in total length (Yao et al.,
346 2022, in press), indicate that the higher-order trophic structure was rebuilt after the EPME.
347 Palaeoecologically, *Hybodus? youngi* displays a heterodont dentition with both high
348 clutching and low grinding teeth, suggesting it was an opportunistic predator that preyed on a
349 broad range of different animals (Cappetta, 2012). The pike-like *Saurichthys* is considered as
350 a large ambush predator with quick strike out of slow movement (Stensiö, 1925; Kogan et al.,

2015, 2020). Thus, large predators with multiple feeding strategies occupied high trophic levels, hinting that the early Ladinian lacustrine ecosystem had longer and more complex food chains than those previously proposed (Zhao et al., 2020).

6. Conclusion

Thirty-one shark teeth were collected from the organic-rich mudstones of Chang 7 at the Bawangzhuang section, Tongchuan City, Shaanxi Province, North China. They are described in details and identified as belonging to two taxa of hybodontiformes, i.e. *Hybodus? youngi* and *Hybodus* sp. The previously poorly described *Hybodus? youngi* is substantially revised based on twenty-nine teeth and a reexamination of the original material and can now be diagnosed by the presence of flared lateral cusplets, an orthodont crown with a pulp cavity surrounded by numerous dentine tubules and a monognathic heterodonty pattern, even if its generic relationships remain problematic. The other hybodont, i.e. *Hybodus* sp., is pending better material for a definite determination. These two hybodonts are proposed as large carnivorous predators in the early Ladinian lacustrine ecosystem of the Ordos Basin. The presence of hybodont sharks and *Saurichthys* occupying high trophic levels in the lake food chains indicates a rebuilding of complex trophic structure in the early Ladinian lacustrine ecosystem of the Ordos Basin following the End Permian Mass Extinction.

Acknowledgements

This study was financially supported by the National Natural Science Foundation of China [No. 41876124, 42172009] and State Key Laboratory of Shale Oil and Gas Enrichment

Mechanisms and Effective Development. We would like to thank Yao Mingtao (student at Peking University) for discussing the Palaeoecology, Dr. Liao Junqi and Geng Binghe (IVPP) for access to the original material of *Hybodus youngi* under their care, Dai Yanlin (student at Peking University) and Zhang Chuanwen (student at China University of Geosciences, Beijing), Yao Zhixiao and Wang Junshe (inhabitants of Bawangzhaung village) for taking part to the field work, and also Hu Tianfen and Wang Mingcui for maintaining the research material in the laboratory. Our reviewers' comments (Michal Ginter and Sebastian Stumpf) greatly improved the quality of the manuscript.

References

Agassiz, J.L.R., (1833–1844; cited as 1837). Recherches sur les poisons fossils. Imprimerie de Petitpierre, Neuchâtel, 1420 pp.

Bengtson, P., 1988. Open nomenclature. Palaeontology 31, 223-227.

Bonaparte, C.L.J., 1838. Selachorum tabula analytica. Nuovi Annali delle Scienze Naturali Bologna 1, 195-214.

Böttcher, R., 2015. Fisches des Lettenkeupers. In: Hagdorn, H., Schoch, R., and Schweigert, G. (Eds.), Der Lettenkeuper - Ein Fenster in die Zeit vor den Dinosauriern. Staatliches Museum für Naturkunde Stuttgart, Stuttgart, pp. 141-202.

Bratvold, J., Delsett, L.L., Hurum, H.J., 2018. Chondrichthyans from the Grippia bonebed (Early Triassic) of Marmierfjellet, Spitsbergen. Norwegian Journal of Geology 98, 189-217.

393 Cappetta, H., 2012. Chondrichthyes (Mesozoic and Cenozoic Elasmobranchii: Teeth):
394 Handbook of Paleoichthyology, Volume 3E. Verlag Dr, Friedrich Pfeil, München, 512
395 pp.
396 Case, G.R., 1978. A new selachian fauna from the Judith River Formation (Campanian) of
397 Montana. Palaeontograpphica, Abt 160(1-6), 176-205.
398 Casini, M., Blenckner, T., Möllmann, C., Gärdmark, A., Lindegren, M., Liope, M., Kornilovs,
399 G., Plikshs, M., Stenseth, N.C., 2012. Predator transitory spillover induces trophic
400 cascades in ecological sinks. Proc Natl Acad Sci USA 109(21), 8185-8189.
401 Chen, Z.Q., Benton, M.J., 2012. The timing and pattern of biotic recovery following the
402 end-Permian mass extinction. Nature Geoscience 5, 375-383.
403 Cupello, C.D., Bermúdez-Rochas, D.D., Martill, D.M., Brito, PM., 2012. The
404 hybodontiformes (chondrichthyes: elasmobranchii) from the missão velha formation
405 (?Lower Cretaceous) of the Araripe Basin, north-east brazil. Comptes Rendus Palevol
406 11(1), 41-47.
407 Delsate, D., Duffin, C.J., Weis, R., 2002. A new microvertebrate fauna from the Middle
408 Hettangian (early Jurassic) of Fontenoille (Province of Luxembourg, South Belgium).
409 Memoirs Geol Surv Belgium 48, 1-84.
410 Deng, S.H., Lu, Y.Z., Luo, Z., Fan, R., Li, X., Zhao, Y., Ma, X.Y., Zhu, R.K., Cui, J.W., 2018.
411 Subdivision and age of the Yanchang Formation and the Middle/Upper Triassic
412 boundary in Ordos Basin, North China. Science China 61(10), 1419-1439.
413 Dorka, M., 2003. Teeth of *Polyacrodus* Jaekel, 1889 from the Triassic of the Germanic Basin:
414 Mitt. Mus. Nat. kd. Berl., Geowiss 6, 147-155.

Du, J.M., Zhao, Y.D., Wang, Q.C., Yu, Y.Q., Xiao, H., Xie, X.K., Du, Y.G., Su, Z.M., 2019. Geochemical characteristics and resource potential analysis of Chang 7 organic-rich black shale in the Ordos Basin. Geological Magazine 156, 1131-1140.

Ginter, M., Hairapetian, V., Klug, C., 2002. Famennian chondrichthyans from the shelves of North Gondwana. Acta Geologica Polonica 52, 169-215.

Guinot, G., Adnet, S., Cavin, L., Cappetta, H., 2013. Cretaceous stem chondrichthyans survived the end–Permian mass extinction. Nature Communications 4, 1-8.

Hairapetian, V., Ginter, M., 2009. Famennian chondrichthyan remains from the Chahriseh section, central Iran. Acta Geologica Polonica 59, 173-200.

Hay, O.P., 1902, Bibliography and catalogue of the fossil vertebrata of North America: United States Geological Survey, Bulletin, 179, pp. 18-68.

Hodnett, J.P.M., Grogan, E., Lund, R., Lucas, S.G., Suazo, T., Elliott, D., Pruitt, J., 2021. Ctenacanthiform sharks from the late Pennsylvanian (Missourian) Tinajas Member of the Atrasado formation, central New Mexico. In: Lucas, G., DiMichele, A., and Allen, D. (Eds.), Kinney Brick Quarry Lagerstätte. New Mexico Museum of Natural History and Science Bulletin 84, 391-424.

Huxley, T.H., 1880. On the application of the laws of evolution to the arrangement of the Vertebrata, and more particularly of the Mammalia: Proceedings of the Zoological Society of London 1880, 649-662.

IGCAGS (Institute of Geology, Chinese Academy of Geological Sciences)., 1980, Mesozoic Stratigraphy and Paleontology of Ordos Basin. Beijing: Geological Publishing House 212 pp. (in Chinese)

437 Jambura, P.L., Türtscher, J., Kindlimann, R., Metscher, B., Pfaff, C., Stumpf, S., Weber, G.W.,
438 Kriwet, J., 2020. Evolutionary trajectories of tooth histology patterns in modern sharks
439 (Chondrichthyes, Elasmobranchii). Journal of Anatomy 236, 753-771.
440 Jin, F., 2006. An overview of Triassic fishes from China. Vertebrata PalAsiatica 44(1), 28-42.
441 Kato, T., Hasegawa, K., Ishibashi, T., 1995. Discovery of early Triassic hybodontoid shark
442 tooth from the southern kitakami massif. Journal of the Geological Society of Japan
443 101(6), 466-469.
444 Kogan, I., Pacholak, S., Licht, M., Schneider, J.W., Brücker, C., Brandt. S., 2015. The
445 invisible fish: hydrodynamic constraints for predator-prey interaction in fossil fish
446 Saurichthys compared to recent actinopterygians. Biology Open 4(12), 1715-1726.
447 Kogan, I., Tintori, A., Iicht, M., 2020. Locomotor function of scales and axial skeleton in
448 Middle-Late Triassic species of *Saurichthys* (Actinopterygii). Rivista Italiana di
449 Paleontologia e Stratigrafia 126(2), 475-498.
450 Kriwet, J., Benton, M.J., 2004. Neoselachian (Chondrichthyes, Elasmobranchii) diversity
451 across the Cretaceous Tertiary boundary. Palaeogeography, Palaeoclimatology,
452 Palaeoecology 214, 181-194.
453 Laojumpon, C., Matkhammee, T., Wathanapitaksakul, A., Suteethorn, V., Suteethorn, S.,
454 Lauprasert, K., Srisuk, P., Le Loeuff, J., 2012. Preliminary report on coprolites from the
455 Late Triassic of Thailand. New Mexico Museum of Natural History and Science 57,
456 207-213.
457 Li, Y., Yao, J.X., Wang, S.E., Pang, Q.Q., 2016. Middle-Late Triassic terrestrial strata and
458 establishment of stages in the Ordos Basin. Acta Geologica Sinica (English Edition) 37,

267-276.

Liu, X.T., 1962. Two new *Hybodus* from north Shensi (Shaanxi), China. Vertebrata PalAsiatica 6, 150-156 (in Chinese with English summary).

Liu, Q.Y., Li, P., Jin, Z.J., Sun, Y.W., Hu, G., Zhu, D.Y., Huang, Z.K., Liang, X.P., Zhang, R., Liu, J.Y., 2021. Organic-rich formation and hydrocarbon enrichment of lacustrine shale strata: a case study of Chang 7 Member. Science China Earth Sciences, doi:10.1007/s11430-021-9819-y.

Lu, L.W., Jin, Y.G., Fang, X.S., 2005. A revision of Middle Jurassic *Hybodus houtienensis* Young (Chondrichthyes: Hybodontidae) from Yunnan. Geol Bull China 24(2), 145-148 (in Chinese with English summary).

Maisch, M.W., Matzke, A.T., 2016. A new hybodontid shark (chondrichthyes, hybodontiformes) from the Lower Jurassic Posidonienschiefer Formation of Dotternhausen, SW Germany. Neues Jahrbuch Für Geologie Und Palontologie Abhandlungen 280(3), 241-257.

Maisey, J.G., 1983. Cranial anatomy of *Hybodus basanus* Egerton from the Lower Cretaceous of England. American Museum Novitates 2758, 1-26.

Maisey, J.G., 1987. Cranial anatomy of the Lower Jurassic shark *Hybodus reticulatus* (Chondrichthyes: Elasmobranchii), with comments on hybodontid systematics. American Museum Novitates 2878, 1-39.

Manzanares, E., Escudero-Mozo, M.J., Ferrón, H., Martínez-Pérez, C., Botella, H., 2020. Middle Triassic sharks from the catalan coastal ranges (NE Spain) and faunal colonization patterns during the westward transgression of Tethys. Palaeogeography,

Palaeoclimatology, Palaeoecology 539, e109489.

Manzanares, E., Pla, C., Ferron, H.G., Botella, H., 2018. Middle-Late Triassic chondrichthyans remains from the Betic Range (Spain). Journal of Iberian Geology, 44, 129-138.

Mutter, R.J., De Blanger, K., Neuman. A.G., 2007. Elasmobranchs from the Lower Triassic Sulphur Mountain Formation near Wapiti Lake (BC, Canada). Zoological Journal of the Linnean Society 149, 309-337.

Mutter, R.J., Neuman, A.G., De Blanger, K., 2008. Homalodontus nom. nov., a replacement name for *Wapitiodus* Mutter, de Blanger and Neuman, 2007 (Homalodontidae nom nov., ?Hybodontoidea), preoccupied by *Wapitiodus* Orchard, 2005. Zoological Journal of the Linnean Society 154, 419-420.

Owen, R., 1846. Lectures on the comparative anatomy and physiology of the vertebrate animals, delivered at the Royal College of Surgeons of England in 1844 and 1846. Part 1. Fishes: Longman, London, 308 pp.

Patterson, C., 1966. British Wealden sharks. Bull Brit Mus (Nat Hist) Geol 11, 283-349.

Qiu, X.W., Liu, C.Y., Mao, G.Z., Deng, Y., Wang, F.F., 2010. Enrichment feature of thorium element in tuff interlayers of Upper Triassic Yanchang formation in Ordos basin, China. Geological Bulletin of China 29(8), 1185-1191 (in Chinese with English abstract).

Qiu, X.W., Liu, C.Y., Wang, F.F., Mao, D., Yu, G.Z., 2015. Trace and rare earth element geochemistry of the Upper Triassic mudstones in the Southern Ordos Basin, Central China. Geological Journal 50, 399-413.

Rees, J., 2008. Interrelationships of Mesozoic hybodont sharks as indicated by dental

503 morphology - preliminary results. Acta Geologica Polonica 58, 217-221.
504 Rieppel, O., Kindlimann, R., Bucher, H., 1996. A new fossil fish fauna from the Middle
505 Triassic (Anisian) of North-Western Nevada. In: Arratia, G., Viohl G. (Eds.), "Mesozoic
506 fishes Systematics and paleoecology", 501-512.
507 Scheyer, T.M., Romano, C., Jenks, J., Bucher, H., 2014. Early Triassic marine biotic
508 recovery,the predators' perspective. PLoS One 9(3), e88987.
509 Shang, Q., Cuny, G., Chen, L., 2008. Early Middle Jurassic vertebrate microremains from the
510 Three Gorges area, southern China. Historical Biology 20(2), 87-99.
511 Steneck, R.S., 2012. Apex predators and trophic cascades in large marine ecosystems:
512 Learning from serendipity. Proceedings of the National Academy of Sciences 109(21),
513 7953-7954.
514 Stensiö, E., 1925. Triassic fishes from Spitzbergen 2: K Sven Vetenskapsakad Handl 3, 1-261.
515 Stumpf, S., Lopez-Romero, F., Kindlimann, R., Lacombat, F., Burkhard, P., Kriwet, J., 2021.
516 A unique hybodontiform skeleton provides novel insights into Mesozoic chondrichthyan
517 life. Papers in Palaeontology 7, 1479-1505.
518 Wang, N.Z., 1977. The Jurassic fish fossils from Liling-Hengyong region of Hunan and its
519 biostratigraphical signifificance. Vertebr PalAsiatica 15(4), 233-243 (in Chinese).
520 Wang, N.Z., Zhang, X., Zhu, M., Zhao, W.J., 2009. A new articulated hybodontoid from late
521 permian of northwestern China. Acta Zoologica 90(S1), 159-170.
522 Winkler, T.C., 1880. Description de quelques restes de poissons fossiles des terrains
523 triasiques des environs de Wurzbourg. Archives du Musée Teyler 5, 109-149.
524 Xue, X.X., 1980. New materials of Hybodontidae in Gansu and Shaanxi. Vertebrata

PalAsiatica 18, 9-15 (in Chinese with English abstract).

Yao, M.T., Sun Z.Y., Meng, Q.Q., Li J.C., Jiang D.Y., 2022. Vertebrate coprolites from Middle Triassic Chang 7 Member in Ordos Basin, China: Palaeobiological and palaeoecological implications. In press, doi：10.1016/j.palaeo.2022.111084.

Yang, H., Fu, J., Yuan, X., 2016. Atlas of Geological Sections of Southern Margin of Ordos Basin: Petroleum Industry Press, Beijing, 503 pp. (in Chinese).

Yang, H., Li, S.X., Liu, X.Y., 2013. Characteristics and resource prospects of tight oil and shale oil in Ordos basin. Acta Petrolei Sinica 34, 1-11 (in Chinese with English abstract).

Yang, Z.Y., Zhang, S.X., Yang, J.D., Zhou, H.Q., Cao, H.S., 2000. Stratigraphy of China: Triassic. Geological Publishing House, Beijing, 138 pp. (in Chinese).

Zhang, J.Y., 2007. Two shark finspines (Hybodontoidea) from the Mesozoic of North China. Cretaceous Research 28, 277-280.

Zhao, X.D., Zheng, D.R., Xie, G.W., Jenkyns, H.C., Guan, C.G., Fang, Y.N., Yuan, X.Q., Xue, N.H., Wang, H., Li, S., Jarzembowski, E.A., Zhang, H.C., Wang, B., 2020. Recovery of lacustrine ecosystems after the end-Permian mass extinction. Geology 48, 109-613.

Figure captions

Figure 1. (A) geographical map of the Ordos basin; (B) close up of the rectangular frame in A, showing the location (yellow star) of the Bawangzhuang locality, Jinsuoguan Town, Tongchuan City; (C) stratigraphic column showing lithologies, fossil shark horizon and U-Pb isotopic ages (Zhao et al., 2020); (D) photograph of shark-yielding strata (Chang 7 Member) at Bawangzhuang section, yellow dash lines represent the mudstone where shark teeth and coprolites were recovered.

548 **Figure 2.** Photograph and diagrammatic sketch of *Hybodus? youngi* from Chang 7 Member,
549 Yanchang Formation, middle Triassic of the Bawangzhuang section: (A-B) parasymphysial
550 teeth?, (A) GMPKU-P-3642a; (B) GMPKU-P-3620; (C-I) anterolateral teeth, (C)
551 GMPKU-P-3619a; (D) GMPKU-P-3648a; (E) GMPKU-P-3646a; (F) GMPKU-P-3643a; (G)
552 GMPKU-P-3661; (H) GMPKU-P-3615a; (I) GMPKU-P-3651; (J-S) posterolateral teeth, (J)
553 GMPKU-P-3644a; (K) GMPKU-P-3649b; (L) GMPKU-P-3650; (M) GMPKU-P-3617a; (N)
554 GMPKU-P-3654b; (O) GMPKU-P-3625; (P) GMPKU-P-3613a; (Q) GMPKU-P-3652a; (R)
555 GMPKU-P-3645b; (S) GMPKU-P-3627. All scale bars represent 1 mm. (C, G, L, O, R, S)
556 labial views; (J, K) apical views. Green represents the enameloid; gray represents the dentine;
557 pink represents the pulp cavity and canal; yellow lines represent ornamentation ridges; black
558 lines represent the dentine tubules.
559 **Figure 3.** (A-F) Histology of *Hybodus? youngi* from Chang 7 Member, Yanchang Formation,
560 middle Triassic of the Bawangzhuang section: (A-C) posterolateral tooth, GMPKU-P-3649b,
561 cross section of the main cusp, (A) second Electron (SE) and (B) back Scattered Electron
562 (BSED) images; (C) enlargement of the enameloid layer at the yellow circle in A, B; (D-F)
563 parasymphysial tooth?, GMPKU-P-3642a, (D) apex of the main cusp with dentine tubules
564 and enameloid layer; (E) vascular canals and pulp cavity of the main cusp; (F) enlargement of
565 the enameloid layer at the yellow circle in E. (G-L) Type specimens: (G-I), *Hybodus? youngi*
566 Liu, 1962 from Yanchang Formation, upper Triassic?, Zhangjiatan, Yanchang County,
567 Shaanxi Province: (G) IVPP V 1042.1 (the holotype); (H) IVPP V 1042.2 and (I) IVPP V
568 1042.3 (paratypes); (J) *Hybodus antingensis* Liu, 1962 from Anding Formation, middle
569 Jurassic, Zhuanwayao, Ansai County, Shaanxi Province, holotype, IVPP V1041; (K-L)

570 *Hybodus huangnidanensis* Wang, 1977 from Huangnitang, Qiyang County, Hunan Province;
571 (K) IVPP V 5223.1 (the holotype); (L) IVPP V 5223.2 (paratype). Scale bars are (A, B, D, E)
572 500 μm; (C, F) 20 μm; (G-L) 1 mm. Green represents the enameloid; gray represents the
573 dentine; pink represents the pulp cavity and canal; yellow lines represent ornamentation
574 ridges.
575 **Figure 4.** Photograph and diagrammatic sketch of *Hybodus* sp. from Chang 7 Member,
576 Yanchang Formation, middle Triassic of the Bawangzhuang section: (A) GMPKU-P-3653a;
577 (B) GMPKU-P-3653b; (C) GMPKU-P-3660. All scale bars represent 1 mm. Green represents
578 the enameloid; gray represents the dentine; pink represents the pulp cavity and canal; yellow
579 lines represent ornamentation ridges.

Figure captions

Figure 1. (A) geographical map of the Ordos basin; (B) close up of the rectangular frame in A, showing the location (yellow star) of the Bawangzhuang locality, Jinsuoguan Town, Tongchuan City; (C) stratigraphic column showing lithologies, fossil shark horizon and U-Pb isotopic ages (Zhao et al., 2020); (D) photograph of shark-yielding strata (Chang 7 member) at Bawangzhuang section, yellow dash lines represent the mudstone where shark teeth and coprolites were recovered.

Figure 2. Photograph and diagrammatic sketch of *Hybodus ? youngi* from Chang 7 Member, Yanchang Formation, middle Triassic of the Bawangzhuang section: (A-B) parasymphysial teeth?, (A) GMPKU-P-3642a; (B) GMPKU-P-3620; (C-I) anterolateral teeth, (C) GMPKU-P-3619a; (D) GMPKU-P-3648a; (E) GMPKU-P-3646a; (F) GMPKU-P-3643a; (G) GMPKU-P-3661; (H) GMPKU-P-3615a; (I) GMPKU-P-3651; (J-S) posterolateral teeth, (J) GMPKU-P-3644a; (K) GMPKU-P-3649b; (L) GMPKU-P-3650; (M) GMPKU-P-3617a; (N) GMPKU-P-3654b; (O) GMPKU-P-3625; (P) GMPKU-P-3613a; (Q) GMPKU-P-3652a; (R) GMPKU-P-3645b; (S) GMPKU-P-3627. All scale bars represent 1 mm. (C, G, L, O, R, S) labial views; (J, K) apical views. Green represents the enameloid; gray represents the dentine; pink represents the pulp cavity and canal; yellow lines represent ornamentation ridges; black lines represent the dentine tubules.

Figure 3. (A-F) Histology of *Hybodus ? youngi* from Chang 7 Member, Yanchang Formation, middle Triassic of the Bawangzhuang section: (A-C) posterolateral tooth,

GMPKU-P-3649b, cross section of the main cusp, (A) second Electron (SE) and (B) back Scattered Electron (BSED) images; (C) enlargement of the enameloid layer at the yellow circle in A, B; (D-F) parasymphysial tooth?, GMPKU-P-3642a, (D) apex of the main cusp with dentine tubules and enameloid layer; (E) vascular canals and pulp cavity of the main cusp; (F) enlargement of the enameloid layer at the yellow circle in E. (G-L) Type specimens: (G-I), *Hybodus ? youngi* Liu, 1962 from Yanchang Formation, upper Triassic?, Zhangjiatan, Yanchang County, Shaanxi Province: (G) IVPP V 1042.1 (the holotype); (H) IVPP V 1042.2 and (I) IVPP V 1042.3 (paratypes); (J) *Hybodus antingensis* Liu, 1962 from Anding Formation, middle Jurassic, Zhuanwayao, Ansai County, Shaanxi Province, holotype, IVPP V1041; (K-L) *Hybodus huangnidanensis* Wang, 1977 from Huangnitang, Qiyang County, Hunan Province; (K) IVPP V 5223.1 (the holotype); (L) IVPP V 5223.2 (paratype). Scale bars are (A, B, D, E) 500 μm; (C, F) 20 μm; (G-L) 1 mm. Green represents the enameloid; gray represents the dentine; pink represents the pulp cavity and canal; yellow lines represent ornamentation ridges.

Figure 4. Photograph and diagrammatic sketch of *Hybodus* sp. from Chang 7 Member, Yanchang Formation, middle Triassic of the Bawangzhuang section: (A) GMPKU-P-3653a; (B) GMPKU-P-3653b; (C) GMPKU-P-3660. All scale bars represent 1 mm. Green represents the enameloid; gray represents the dentine; pink represents the pulp cavity and canal; yellow lines represent ornamentation ridges.

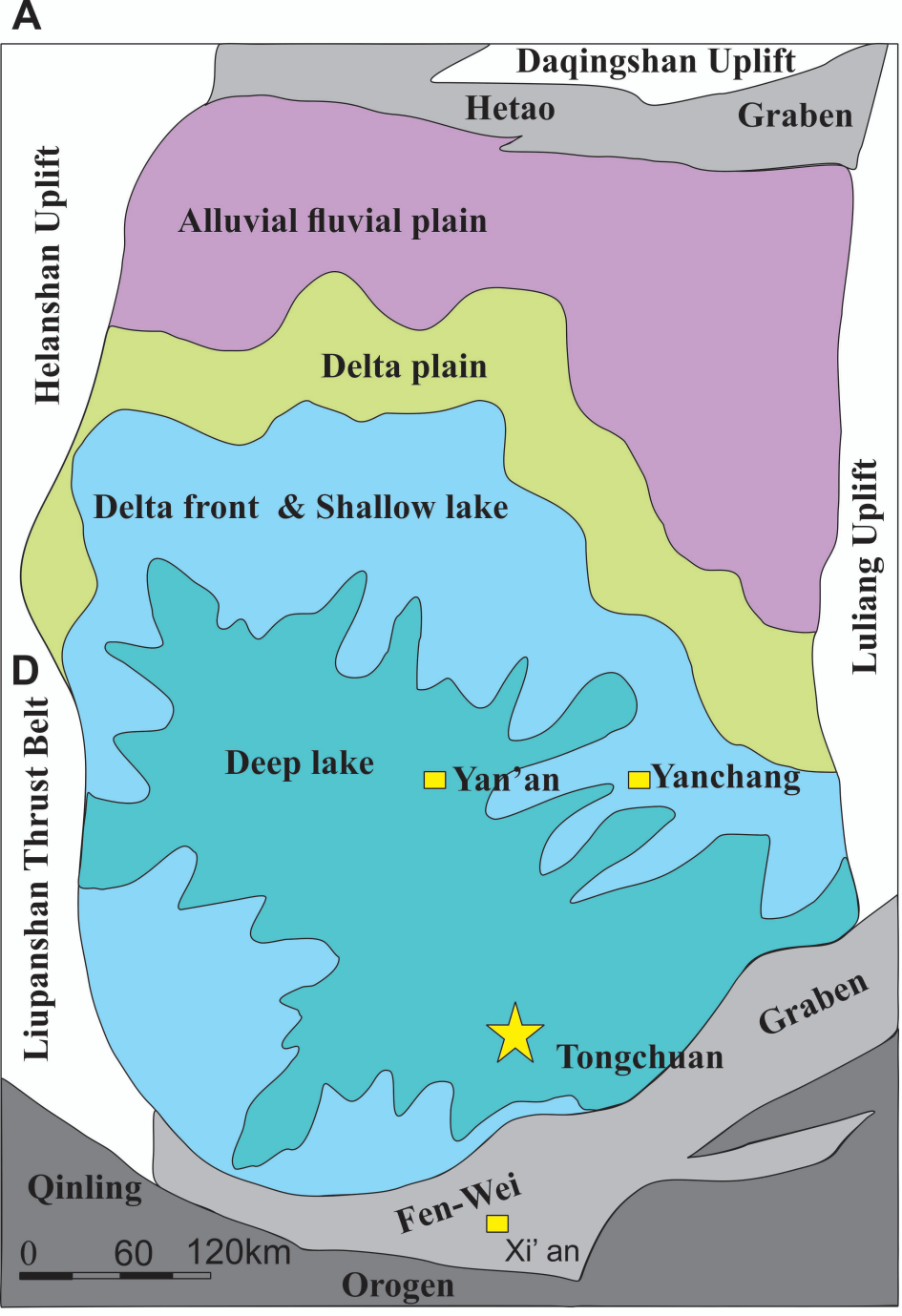
A
Daqingshan Uplift
Hetao
Graben
Helanshan Uplift
Alluvial fluvial plain
Delta plain
Delta front & Shallow lake
Luliang Uplift
D
Deep lake
Yan'an
Yanchang
Liupanshan Thrust Belt
Tongchuan
Graben
Qinling
Fen-Wei
Xi' an
0 60 120km
Orogen


C

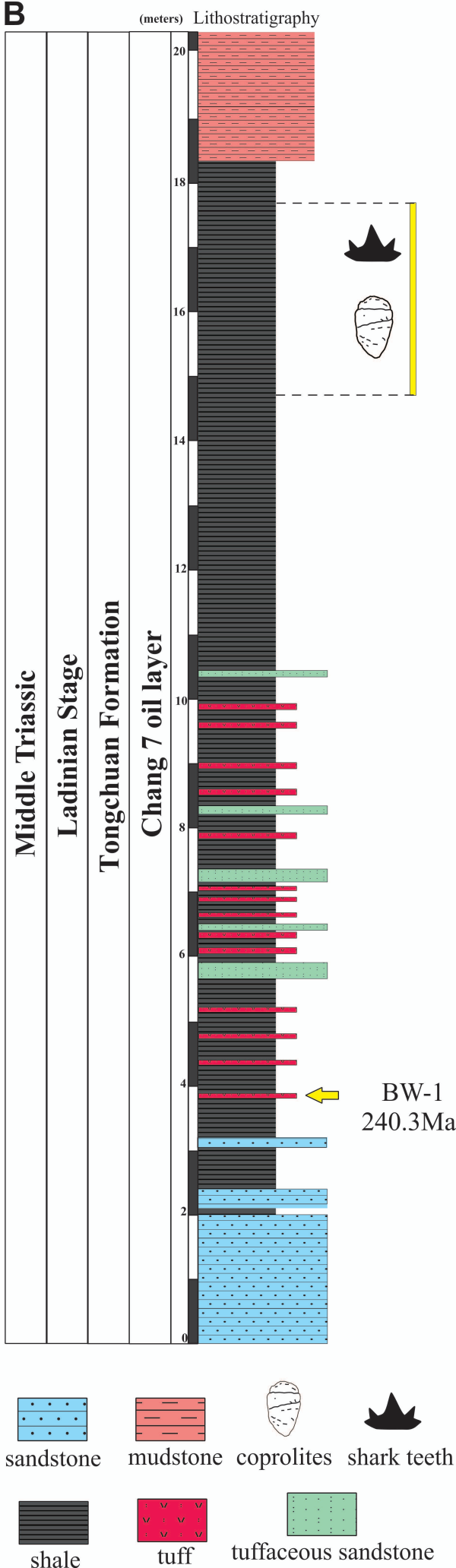
B
(meters)
Lithostratigraphy
Middle Triassic
Ladinian Stage
Tongchuan Formation
Chang 7 oil layer
20
18
16
14
12
10
8
6
4
2
0
BW-1
240.3Ma
sandstone
mudstone
coprolites
shark teeth
shale
tuff
tuffaceous sandstone

Parasymphysial teeth ?

Anterolateral teeth ?

Posterolateral teeth ?

A

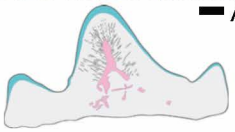

B

Hybodus youngi

the main cusp of *Hybodus youngi*

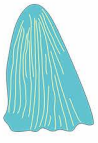

I

C

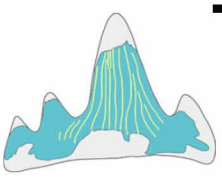

E

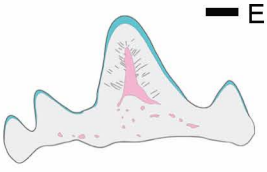

G

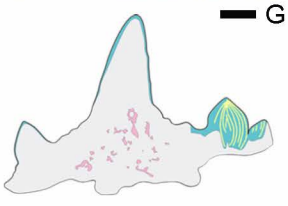

D

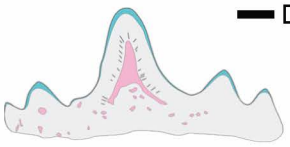

F

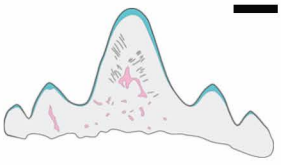

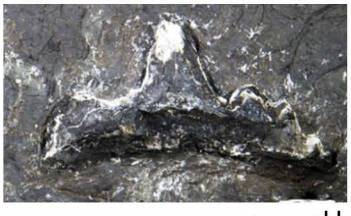

H

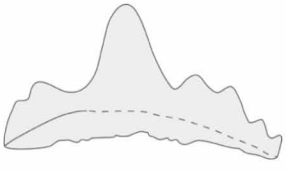

L

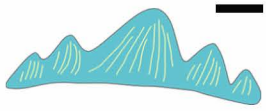

M

N

O

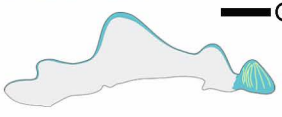

P

Hybodus aff. *antingensis*

J

K

S

R

Q

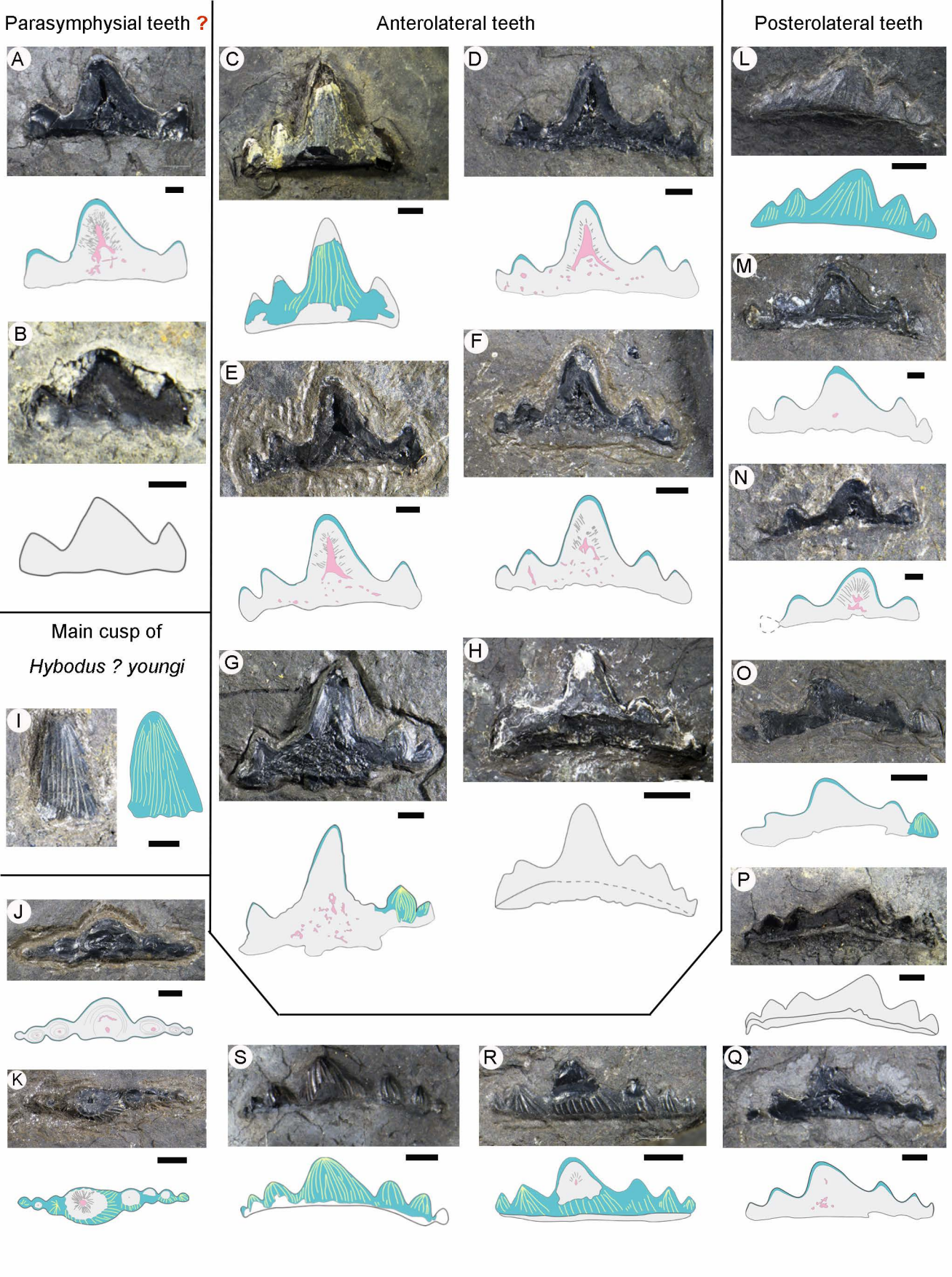
Parasymphysial teeth ?
Anterolateral teeth
Posterolateral teeth
A
B
C
D
E
F
G
H
L
M
N
O
P
Q
R
S
Main cusp of
Hybodus ? youngi
I
J
K

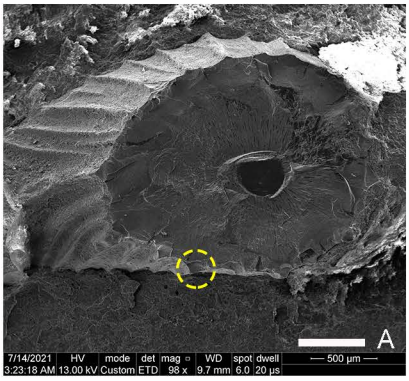
A
7/14/2021 HV mode det mag WD spot dwell
3:23:18 AM 13.00 kV Custom ETD 98 x 9.7 mm 6.0 20 µs
500 µm

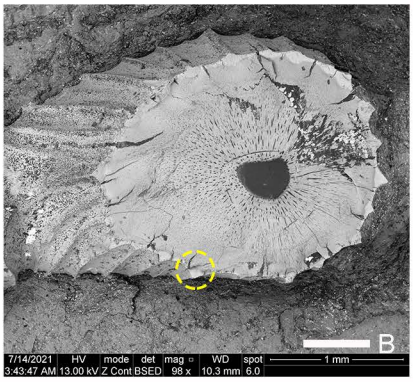
B
7/14/2021 HV mode det mag WD spot
3:43:47 AM 13.00 kV Z Cont BSED 98 x 10.3 mm 6.0
1 mm

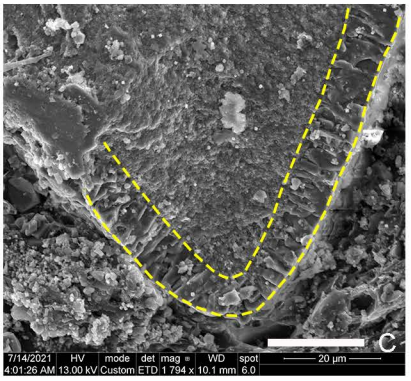
C
7/14/2021 HV mode det mag WD spot
4:01:26 AM 13.00 kV Custom ETD 1 794 x 10.1 mm 6.0
20 µm

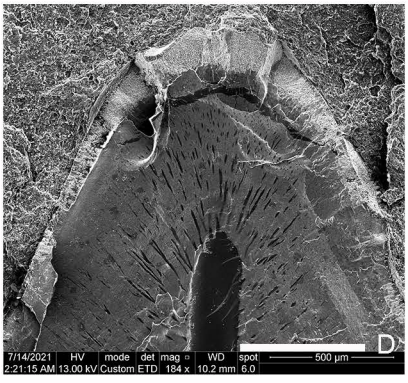
D
7/14/2021 HV mode det mag WD spot
2:21:15 AM 13.00 kV Custom ETD 184 x 10.2 mm 6.0
500 µm

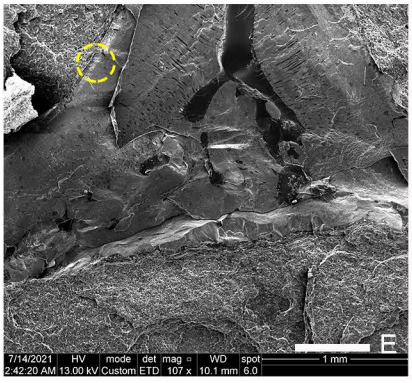
E
7/14/2021 HV mode det mag WD spot
2:42:20 AM 13.00 kV Custom ETD 107 x 10.1 mm 6.0
1 mm

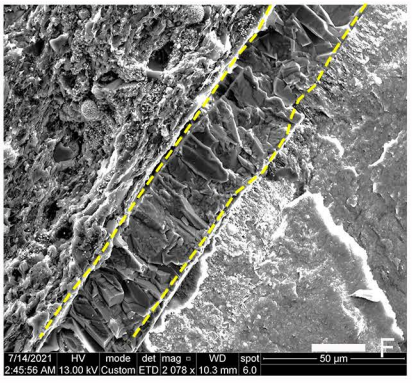
F
7/14/2021 HV mode det mag WD spot
2:45:56 AM 13.00 kV Custom ETD 2 078 x 10.3 mm 6.0
50 µm


G


H

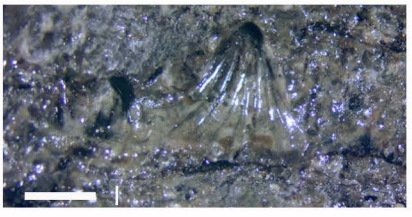
I

G´

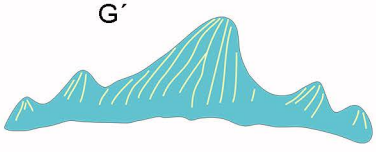

H´

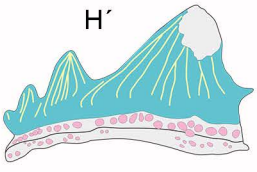

I´

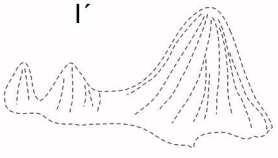

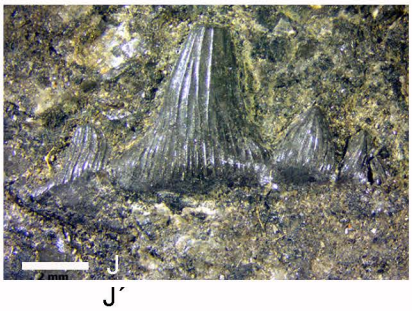
J

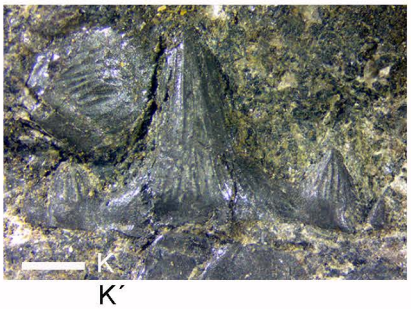
K


L

J´

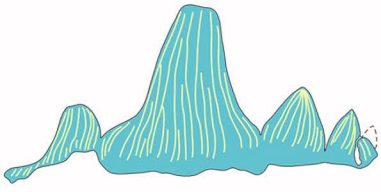

K´

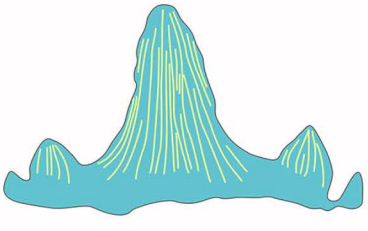

L´

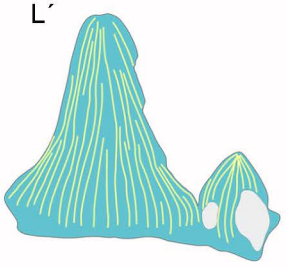

A

B

C

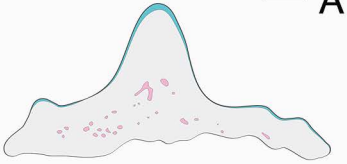

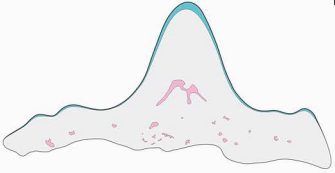

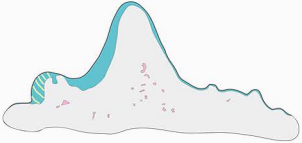

Appendix 1

Results of the EDS analyses of the sediments in the pulp cavity of the *Hybodus ? youngi*

Specimen: parasymphysial tooth? GMPKU-P-3642a (see Fig 3.4)

Spectrum processing :
Peak possibly omitted : 3.710 keV

Processing option : All elements analyzed (Normalised)
Number of iterations = 4

Standard :
C CaCO3 1-Jun-1999 12:00 AM
O SiO2 1-Jun-1999 12:00 AM
S FeS2 1-Jun-1999 12:00 AM

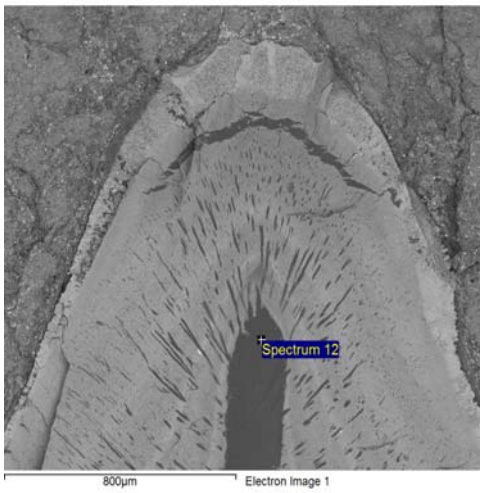

Element	Weight %	Atomic %
C K	73.61	79.20
O K	25.10	20.27
S K	1.30	0.52
Totals	100.00	

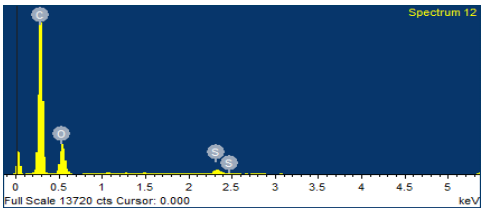

Specimen: posterolateral tooth, GMPKU-P-3649b (see Fig 2.11)

Spectrum processing :
Peak possibly omitted : 1.051 keV

Processing option : All elements analyzed (Normalised)
Number of iterations = 4

Standard :
C CaCO3 1-Jun-1999 12:00 AM
O SiO2 1-Jun-1999 12:00 AM
S FeS2 1-Jun-1999 12:00 AM
Ca Wollastonite 1-Jun-1999 12:00 AM

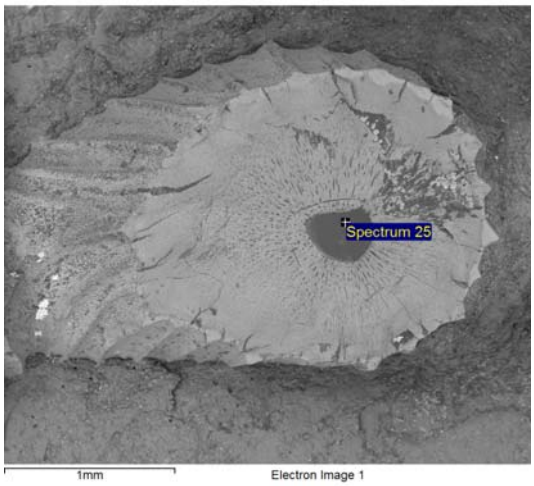

Element	Weight %	Atomic %
C K	71.41	77.26
O K	27.43	22.28
S K	0.94	0.38
Ca K	0.22	0.07
Totals	100.00